The IEE Power Conversion & Applications Professional Network

Finite Element Analysis of Single Turn Coil Systems for Ultrahigh Magnetic Field Production

D F Rankin, B M Novac &
I R Smith,
Loughborough University

Printed and published by the IEE, Michael Faraday House, Six Hills Way,
Stevenage, Herts SG1 2AY, UK

Abstract

This paper describes the implementation of an advanced computational technique in predicting the production of ultrahigh magnetic fields by single-turn coil systems energised by the discharge current of a capacitor. By taking full account of the complex magnetic, thermal and structural interactions that are present, a tool is provided for accurately analysing and optimising the performance of practical systems.

The use of a complete multiphysical finite element model enables both the peak flux density produced by small destructive systems and the complete dynamics of larger and non-destructive electro-plastic systems to be very accurately predicted. Descriptions are given of a number of experiments with widely different geometries, that provide a broad spectrum on which the model was validated. In particular, the full information that is available from the model is illustrated by considerations of a shown in considerations of a non destructive but highly plastic deformation experiment.

This work is highly relevant to electromagnetic metal forming techniques in industry.

FINITE ELEMENT ANALYSIS OF SINGLE TURN COIL SYSTEMS FOR ULTRAHIGH MAGNETIC FIELD PRODUCTION

D. F. Rankin, B. M. Novac, and I. R. Smith[ξ]

Department of Electronic and Electrical Engineering, Loughborough University, UK
[ξ]email: I.R.Smith@lboro.ac.uk

Keywords: Finite element analysis, pulsed power, ultrahigh magnetic fields.

Abstract

Accurate modelling of pulsed magnetic field systems finds an important application in accurately predicting the magnetic flux density and forces that are generated This paper presents a detailed three-dimensional finite element model for use with single turn coil systems producing ultrahigh magnetic fields and compares simulated solutions with reliable experimental data.

1. Introduction

Recent work at Loughborough has seen the successful development of an accurate multiphysical three dimensional finite element model of elasto-plastic metallic deformation under the application of fast transient currents, Rankin et al [1] Results from this detailed work have important potential applications in such sectors as metal forming, Psyk et al [2], and for magnetic field systems and associated conditioning components.

Previous considerations involving finite element analysis (FEA) have focused on the modelling of systems in which the forces produced are insufficient to cause the metallic structure to be destroyed, and the complex transient physical phenomena associated with high-powered ultrahigh magnetic field systems do not play an influential role. The work presented in this paper highlights the application of a more complete FEA approach to the performance prediction when ultrahigh fields (>100T) are produced and in particular to systems based on a destructive single-turn coil (STC). Electromagnetic, structural and thermal effects are all taken into account and, although limitations exist, a comparison between predicted and measured results serve to highlight the accuracy of the simulation in predicting the peak fields produced in practice.

2. Single turn coil systems

Single turn coil systems, as shown typically in Figure 1, are used as a laboratory tool for producing pulsed ultrahigh magnetic fields, Portugall et al [3]. Switch S is closed when the high energy capacitor bank C is charged to an initial high voltage V_0, to discharge the electrostatically stored energy into the coil through the flat parallel-plate transmission line of inductance L_T and resistance R_T. The resulting current I_C rises rapidly, and eventually produces a high magnetic flux density at the centre of the STC that is related to the energy initially stored and the geometric size of the system, and is inversely related to the overall inductance of the circuit. During the capacitor discharge, the electromagnetic Maxwell tensor (magnetic pressure) acting on the STC produces 3D deformation.

When the magnetic flux density produced exceeds about 100T the forces generated may be sufficiently large to result in destruction of the coil, while various high energy/high temperature phenomena such as shock waves, non-linear magnetic diffusion and surface vaporisation may also be present.

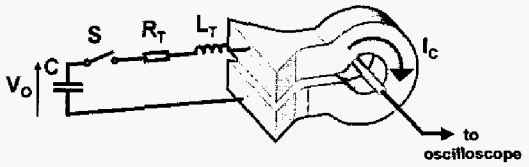

Figure 1. Experimental STC arrangement, R_T and L_T include all circuit resistances and inductances other than the STC

Table 1 details two high-powered destructive STC systems available at Loughborough. Both have been used to benchmark the accuracy of the FEA model described below, by predicting the history of the magnetic field that is produced.

	COIL GEOMETRY			EXTERNAL CIRCUITRY			
DESIGN	Inner Radius (mm)	Outer Radius (mm)	Height (mm)	C (μF)	V_0 (kV)	R_T (mΩ)	L_T (nH)
A	1.5	2.5	4.9	56.64	25.0	9.0	19.1
B	1.0	2.0	2.0	56.64	25.3	7.0	18

Table 1. Data for Loughborough STC experiments. All STCs made from copper.

3. Multiphysical finite element analysis

In order to obtain a true understanding of the complexity of pulsed electromagnetic loading in a STC it is necessary to consider all the physical interactions that occur, and this is ensured at Loughborough by employment of the commercial code ANSYS®.

The three main disciplines involved are electromagnetic (EMAG), thermal (THERM) and structural (STRUCT), and these must be solved independently and consecutively throughout a computational solution. During the solution numerical results from one discipline must be passed as loads to the next, as shown in the flow chart of Figure 2. The time interval specified by K increments after each iteration cycle through the solution, until it reaches a specified maximum time that signifies the end of the period of interest.

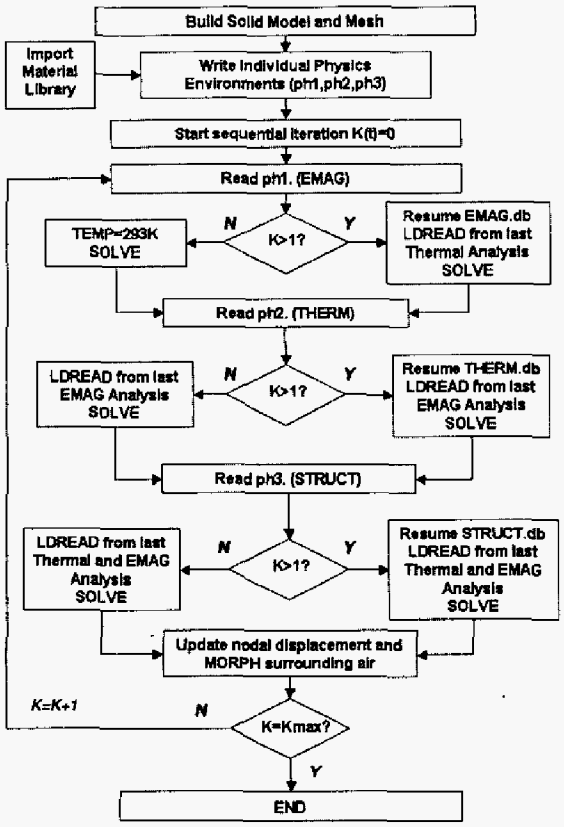

Figure 2. Multiphysical flow chart

The typical topology and the way in which the FEA model is established ar shown in Figure 3, with Figure 3(a) being a topological representation of the STC shown in Figure 1. This solid model can however be simplified by taking advantage of the inherent degrees of symmetry, and Figure 3(b) shows the simplified quarter model used in FEA simulation at Loughborough

Figure 3(c) shows a meshed volume of the quarter-coil and highlights its attachment to the FEA circuit model used in the electromagnetic analysis. By establishing the correct boundary conditions the circuit is able to compute the overall resistance and inductance, as if it were connected to the full model of Figure 3(a). For clarity the mesh shown in Figure 3(c) neglects the air mesh surrounding the coil that includes far-field elements on the outer boundary. These far-field elements model the infinite plane.

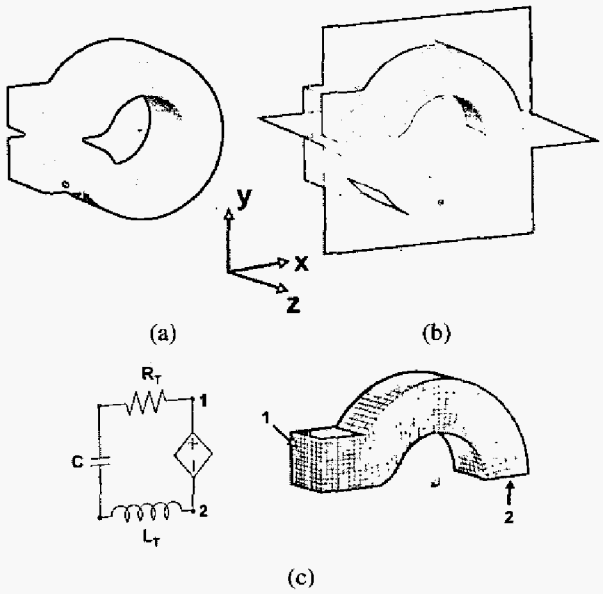

Figure 3: STC Model (a) full solid model (b) quarter model used at Loughborough (c) FEA model

During the simulation, relevant temperature dependant material properties are introduced for each individual environment.. As the temperature approaches that of melting through to vaporisation, data from the SESAME [4] database allows for temperature dependent conductivity prediction within the EMAG environment. Similarly, temperature dependant enthalpy variations are included in the considerations of latent heat absorption within the THERM environment. Phase changes were not however considered in the STRUCT environment. Although this introduces an inherent limitation when implementing the integrated code, it may not play an influential role in the prediction of the peak field produced by an ultrahigh field system.

4. Benchmarking of system model

Using the parameters given in Table 1, the accuracy of the above model in predicting the fields produced by ultrahigh magnetic systems was benchmarked against reliable experimental data.

For the experiment with coil A of Table 1, the mean flux density along the central axis of the STC was measured using a Schott's SF6 high lead glass Faraday rotation sensor, 5 mm long and 1.5 mm^2 in cross section. The cross section of the laser beam through the crystal was reduced by a two-lens system, with the maximum intensity focussed on a circular region about 0.1 mm in diameter. Since however it is difficult to estimate the influence of light outside this region, the active cross section over which the magnetic field contributes to the Faraday rotation was conservatively estimated as a circle 0.3 mm in diameter. It is clear that the predicted magneto-optic effect will therefore be less than that measured Figure 4 compares both the measured and predicted output signals from the probe and the corresponding axial flux densities derived from the Faraday rotation signal.

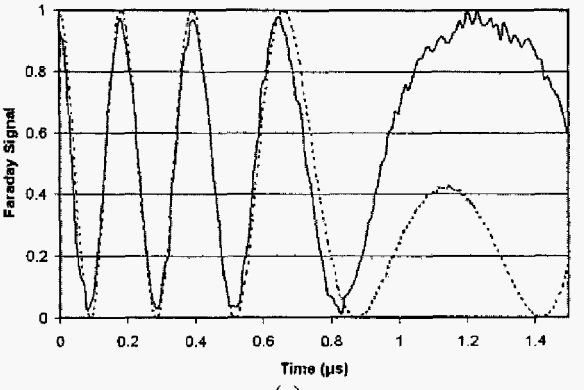

(a)

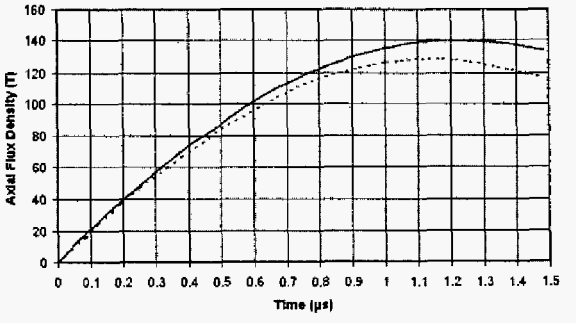

(b)

Figure 4: Coil design Z (a) Faraday rotation signal (in arbitrary units) (b) axial magnetic flux density

——— experimental ····· 3D FEA prediction

The maximum axial flux density of 140 T is produced within 1.25 μs of the switch closure, and the 3D model predicts 129.5 T at the same time. The accuracy of prediction is art all times is within 7%, although most probably shock waves will have affected the crystal in the final two hundred or so nanoseconds before the peak field was produced.

Similarly, Figure 5 compares the measured and predicted 3D time variation of the flux density at the centre of the axis of coil B. In this instance the flux density in the central region of the STC is measured by a magnetic pick up probe having 2 turns on a 1 mm diameter mandrel and having an estimated calibration error of less than 3%. The peak flux density of 240 T occurs about 0.8 μs after closure of switch S.

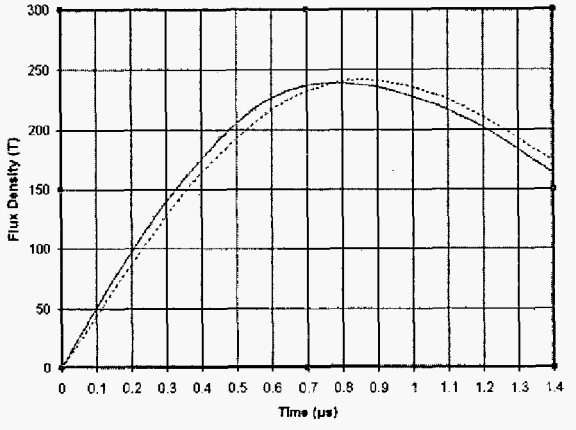

Figure 5: Axial magnetic flux density of coil Y

——— experimental ····· 3D FEA prediction

By using flash X-ray photography the radial dimensions of coil B were recorded at intervals during production of the field shown in Figure 5, enabling a comparison to be made between structural predictions and measurements of the coil dynamics. Due to the experimental set-up required for Faraday rotation measurements, it has not yet been possible to produce similar X-ray images for coil A.

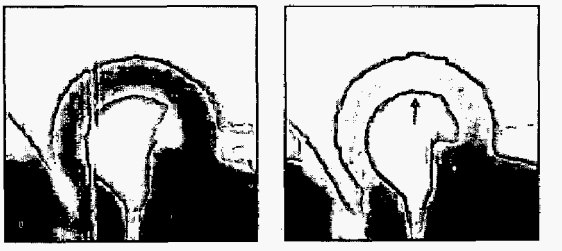

(a)

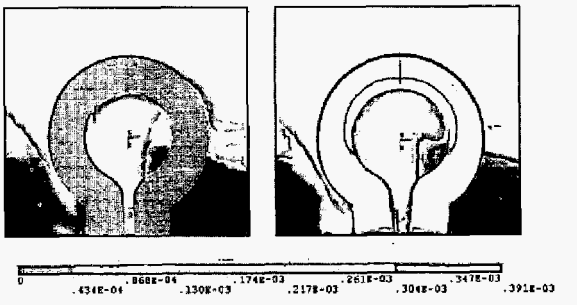

(b)

Figure 6: X-ray dynamics of coil B (a) images at 0 ns and 820 ns (b) corresponding predicted shapes - scale indicates vector displacement in m.

The X-ray pictures of Figure 6(a) shows an end view of coil B prior to the capacitor discharge (left) and 820 ns after switch S is closed (right), very close to the time at which the peak flux density is produced (see Figure 5). It is evident that the coil has begun to expand radially due to the magnetic pressure generated, although this expansion is not homogenous and the area highlighted has travelled furthest. Also obvious is a widening of the gap in the coil at the connection to the transmission system.

In Figure 6(b), predicted end views of the coil are superimposed on experimental recordings, and the correlation clearly shows generally good agreement. Figure 6(a) shows that after 820 ns some necking of the coil has occurred in the lower left section of the coil, which is believed to be attributable to the inhomogeneous construction of the coil and is not replicated in the simulation of Figure 6(b). Beyond a certain time, structural instabilities obviously play an important role in the dynamics of the model, and Figure 7 is an end view of the coil 1200ns after closure of switch S. This is however well beyond both the capabilities of the current model and the time of interest when considering ultrahigh magnetic field production (see Figure 5).

Figure 7: X-ray dynamics coil B at 1200 ns

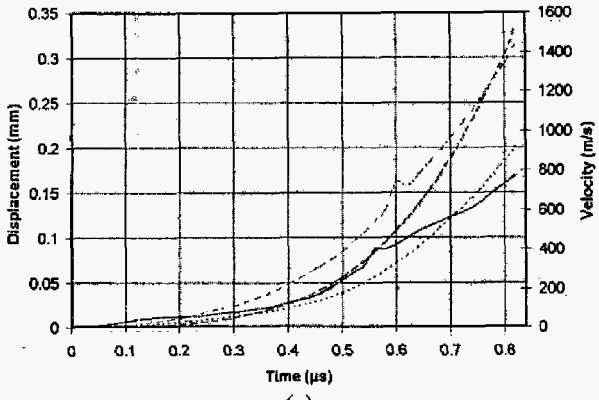

(a)

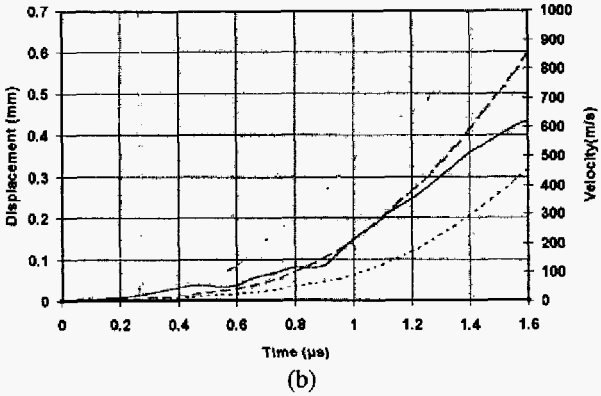

(b)

Figure 8: Predicted dynamics (a) Coil B (b) Coil A

---- radial displacement ····· axial displacement

-·-·- radial velocity —— axial velocity

Figure 8(a) shows the predicted radial and height dynamics of coil B at the point highlighted in Figure 6(a). When the peak field is produced the outer edges have translated almost 0.34 mm radially, reaching predicted speeds in excess of 1500 m/s.

Similarly, Figure 8(b) shows the predicted radial and height dynamics of a corresponding point of coil A. In this case the radial speeds are in excess of 900 m/s, and highlight again the ability of the model to capture accurately the ultrahigh peak field under extreme transient conditions.

5. Conclusion

It has been shown that accurate FEA modelling is possible of single-turn coils producing ultrahigh pulsed magnetic fields. Furthermore it has been confirmed that while limitations arise it is possible to achieve accurate predictions of both peak flux density and coil dynamics. The ability to model such complex system in three dimensions allows for system innovation and more speedy design, and the work is now expanding to include other such pulsed power systems and associated conditioning components.

Acknowledgements

The work described was supported by EPSRC and MoD through their Joint Grant Scheme (Research Grant GR/R 44645) and also by EPSRC through the award of a research studentship to D.F.Rankin.

References

[1] D. F. Rankin , B. M. Novac, and I. R. Smith, "Finite Element Analysis of Magnetic Single Turn Systems", *15th International Pulsed Power Conference, Monterey CA, USA, June 13th – 17th* (2005) to be published.

[2]V. Psyk, C. Beerwald, M. Kleiner, M. Beerwald and A. Henselek, "Use of electromagnetic forming in process combinations for the production of automotive parts", *Proceedings of 2nd European Pulsed Power Symposium, DESY, Hamburg, Germany, 20-23 September*, pp. 82-86. (2004)

[3] O. Portugall, N. Puhlmann, H. U. Muller, M. Barczewski, I. Stolpe and M. van Ortenberg, J.Phys.D:Appl.Phys. 32 pp. 2354-66. (1999)

[4] S. P. Lyon, J. D. Johnson , SESAME: The Los Alamos National Laboratory equation of state data base *Report LA-UR-92-3407*. (1992)